

LPHE Note 2006-011
May 30, 2006

**BEYOND THE STANDARD MODEL AT BELLE: $B \rightarrow K^* \ell^+ \ell^-$
AND SEARCH FOR LEPTONIC B DECAYS**

Stefano Villa

*Laboratory for High-Energy Physics, Ecole Polytechnique Fédérale,
CH-1015 Lausanne, Switzerland*

Abstract

We report the first measurement of the forward-backward asymmetry and the ratios of Wilson coefficients A_9/A_7 and A_{10}/A_7 in $B \rightarrow K^* \ell^+ \ell^-$, obtained using 386M $B\bar{B}$ pairs that were collected at the $\Upsilon(4S)$ resonance with the Belle detector at the KEKB asymmetric-energy e^+e^- collider. We also summarise the results obtained by Belle in searches for purely leptonic B decays, with emphasis on their impact on models of physics beyond the Standard Model.

1 Introduction

The Belle detector ¹⁾, operating at the KEKB e^+e^- collider ²⁾ at a centre-of-mass energy corresponding to the mass of the $\Upsilon(4S)$ resonance, has accumulated as of May 2006 a data sample corresponding to more than 500M $B\bar{B}$ pairs. Such a large sample of B mesons allows the study of rare B decays, which are among the cleanest probes of the flavour sector of the Standard Model (SM) available to present experiments. In particular, these decays have the potential of revealing the existence of new particles and couplings not present in the SM, but predicted by several models of physics Beyond the SM (BSM).

In the last few years Belle has reported several measurements that constrain the parameter space of BSM theories. In particular, this review will concentrate on the measurement of forward-backward asymmetry and of ratios of Wilson coefficients in $B \rightarrow K^*\ell^+\ell^-$ ³⁾, described in Section 2, and on the searches for purely leptonic B decays of the type $B \rightarrow \ell\nu$, detailed in Section 3, and $B^0 \rightarrow \ell^+\ell^-$ (Section 4).

2 Measurement of forward-backward asymmetry and ratios of Wilson coefficients in $B \rightarrow K^*\ell^+\ell^-$

Flavor-changing neutral current $b \rightarrow s$ processes are forbidden at tree level and can only proceed via loop diagrams in the SM. Loops are sensitive to new physics effects via insertion of heavy particles in the internal lines; if new heavy particles can contribute to the decays, their amplitudes will interfere with the SM amplitudes and thereby modify the decay rate as well as differential distributions.

Such contributions would therefore change the Wilson coefficients ⁴⁾ that parametrise the strength of the short distance interactions. The $b \rightarrow s\ell^+\ell^-$ amplitude is described by the effective Wilson coefficients \tilde{C}_7^{eff} , \tilde{C}_9^{eff} and $\tilde{C}_{10}^{\text{eff}}$, whose terms have been calculated up to next-to-next-to-leading order (NNLO) in the SM ⁵⁾. A measurement of the forward-backward asymmetry and of the differential decay rate $g(q^2, \theta) = d^2\Gamma/dq^2 d\cos\theta$ as functions of q^2 and θ for $B \rightarrow K^*\ell^+\ell^-$ constrains the relative signs and magnitudes of these coefficients ^{6, 7)}. Here q^2 is the squared invariant mass of the dilepton system, and θ is the angle between the momenta of the negatively (positively) charged lepton and the B (\bar{B}) meson in the dilepton rest frame. The forward-backward asymmetry is defined as

$$\mathcal{A}_{\text{FB}}(q^2) = \frac{\int_{-1}^1 \text{sgn}(\cos\theta)g(q^2, \theta)d\cos\theta}{\int_{-1}^1 g(q^2, \theta)d\cos\theta}. \quad (1)$$

2.1 Selection of $B \rightarrow K^* \ell^+ \ell^-$ events

The analysis is based on a 357 fb^{-1} data sample containing 386M $B\bar{B}$ pairs; the $B^+ \rightarrow K^+ \ell^+ \ell^-$ mode is also studied, since it is expected to have a very small forward-backward asymmetry even in the presence of new physics⁸⁾ and can therefore be used as null test for the \mathcal{A}_{FB} measurement.

The following final states are used to reconstruct B candidates: $K^{*0} \ell^+ \ell^-$, $K^{*+} \ell^+ \ell^-$, and $K^+ \ell^+ \ell^-$, with subdecays $K^{*0} \rightarrow K^+ \pi^-$, $K^{*+} \rightarrow K_S^0 \pi^+$ and $K^+ \pi^0$, $K_S^0 \rightarrow \pi^+ \pi^-$, and $\pi^0 \rightarrow \gamma\gamma$. Hereafter, $K^{*0} \ell^+ \ell^-$ and $K^{*+} \ell^+ \ell^-$ are combined and called $K^* \ell^+ \ell^-$. Two variables defined in the centre-of-mass (CM) frame are used to select B candidates: the beam-energy constrained mass $M_{\text{bc}} \equiv \sqrt{E_{\text{beam}}^2 - p_B^2}$ and the energy difference $\Delta E \equiv E_B - E_{\text{beam}}$, where p_B and E_B are the measured CM momentum and energy of the B candidate, and E_{beam} is the CM beam energy.

The dominant background consists of $B\bar{B}$ events where both B mesons decay semileptonically. This background is suppressed using missing energy and $\cos\theta_B^*$, where θ_B^* is the angle between the flight direction of the B meson and the beam axis in the CM frame. The resonant contributions due to charmonia (J/ψ and $\psi(2S)$) are rejected using the dilepton invariant mass. The signal box is defined as $|M_{\text{bc}} - m_B| < 8 \text{ MeV}/c^2$ for both lepton modes and $-55 (-35) \text{ MeV} < \Delta E < 35 \text{ MeV}$ for the electron (muon) mode. An unbinned maximum-likelihood fit to the M_{bc} distribution is performed in order to determine the signal yield. The fit includes several event categories, i.e. signal, three types of cross-feeds and four background sources. In the fit, all background fractions except the dilepton background are fixed while the signal fraction is allowed to float.

The fit yields 113.6 ± 13.0 and 96.0 ± 12.0 signal events for the $K^* \ell^+ \ell^-$ and $K^+ \ell^+ \ell^-$ modes, respectively. Data and fit results are shown in Figure 1.

2.2 Extraction of \mathcal{A}_{FB} and Wilson coefficients

The $B \rightarrow K^* \ell^+ \ell^-$ candidates in the signal box are used to measure the normalised double differential decay width. For the evaluation of the Wilson coefficients, the NNLO Wilson coefficients \tilde{C}_i of Ref. 5) are used. Since the full NNLO calculation only exists for $q^2/m_b^2 < 0.25$, we adopt the so-called partial NNLO calculation⁹⁾ for $q^2/m_b^2 > 0.25$. The higher order terms in the \tilde{C}_i are fixed to the SM values while the leading terms A_i , with the exception of A_7 , are allowed to float. Since the branching fraction measurement of $B \rightarrow X_s \gamma$ is consistent with the prediction for $|A_7|$ within the SM, A_7 is fixed at the SM value, -0.330 , or the sign-flipped value, $+0.330$. The fit parameters are therefore A_9/A_7 and A_{10}/A_7 ; the SM predictions for A_9 and A_{10} are 4.069 and -4.213 , respectively⁹⁾.

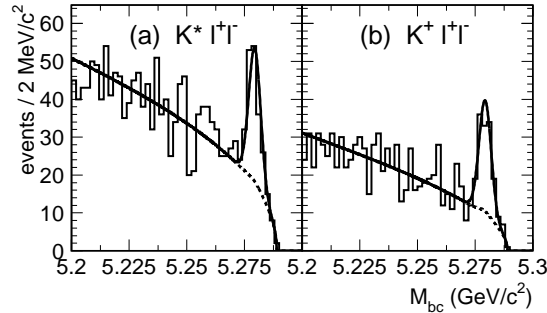


Figure 1: M_{bc} distributions for the (a) $B \rightarrow K^* \ell^+ \ell^-$ and (b) $B \rightarrow K^+ \ell^+ \ell^-$ samples. The solid and dashed curves are the fit results for the total and background contributions, respectively.

To extract these ratios, an unbinned maximum likelihood fit is performed to the events in the signal box with a probability density function that includes the normalised double differential decay width.

The q^2 -integrated asymmetry \tilde{A}_{FB} is measured by determining the yield in forward and backward regions from a fit to the M_{bc} distribution. After correcting for efficiency, the result is:

$$\begin{aligned} \tilde{A}_{FB}(B \rightarrow K^* \ell^+ \ell^-) &= 0.50 \pm 0.15 \pm 0.02, \\ \tilde{A}_{FB}(B^+ \rightarrow K^+ \ell^+ \ell^-) &= 0.10 \pm 0.14 \pm 0.01, \end{aligned} \quad (2)$$

where the first uncertainty is statistical and the second is systematic. A large integrated asymmetry is observed for $K^* \ell^+ \ell^-$ with a significance of 3.4σ . The result for $K^+ \ell^+ \ell^-$ is consistent with zero as expected.

The fit results of ratios of Wilson coefficients are summarised in Table 1. Figure 2 shows the fit results projected onto the background-subtracted forward-backward asymmetry distribution in bins of q^2 .

The fit results are consistent with the SM values $A_9/A_7 = -12.3$ and $A_{10}/A_7 = 12.8$. In Figure 3, we show confidence level (CL) contours in the $(A_9/A_7, A_{10}/A_7)$ plane based on the fit likelihood smeared by the systematic uncertainty, which is assumed to have a Gaussian distribution. We also calculate an interval in $A_9 A_{10}/A_7^2$ at the 95% CL for the allowed A_7 region,

$$-14.0 \times 10^2 < A_9 A_{10}/A_7^2 < -26.4. \quad (3)$$

This result implies that the sign of $A_9 A_{10}$ must be negative, and the solutions

Table 1: A_9/A_7 and A_{10}/A_7 fit results for negative and positive A_7 values. The first uncertainty is statistical and the second is systematic.

	Negative A_7	Positive A_7
A_9/A_7	$-15.3^{+3.4}_{-4.8} \pm 1.1$	$-16.3^{+3.7}_{-5.7} \pm 1.4$
A_{10}/A_7	$10.3^{+5.2}_{-3.5} \pm 1.8$	$11.1^{+6.0}_{-3.9} \pm 2.4$

in quadrants I and III of Figure 3 are excluded at 98.2% CL. Since solutions in both quadrants II and IV are allowed, we cannot determine the sign of $A_7 A_{10}$.

3 Search for $B \rightarrow \ell \nu$

Leptonic decays of charged B mesons proceed in the SM via the W -mediated annihilation tree diagram, with a branching fraction given by:

$$\mathcal{B}(B^+ \rightarrow \ell^+ \nu_\ell) = \frac{G_F^2 m_B}{8\pi} m_\ell^2 \left(1 - \frac{m_\ell^2}{m_B^2}\right)^2 f_B^2 |V_{ub}|^2 \tau_B, \quad (4)$$

where τ_B is the B meson lifetime, f_B is the B decay constant and V_{ub} an element of the CKM-matrix. These modes are thus very interesting because they give direct access to the product $f_B \times V_{ub}$, from which one can extract a measurement of f_B . The SM expectation for $B^+ \rightarrow \tau^+ \nu_\tau$ is around $\mathcal{B}(B^+ \rightarrow \tau^+ \nu_\tau) = 1.0 \times 10^{-4}$; decays to lighter leptons are helicity suppressed, by factors of 223 for muons and 10^7 for electrons. Allowing for decay amplitudes BSM, measurements of these processes give stringent limits on important parameters of such SM extensions, e.g. the mass of the charged Higgs boson and $\tan \beta$ (the ratio of vacuum expectation values of the two Higgs doublets) in the minimal supersymmetric SM (MSSM), or leptoquark masses in Pati-Salam models.

3.1 $B^+ \rightarrow \tau^+ \nu_\tau$

The search for $B^+ \rightarrow \tau^+ \nu_\tau$ ¹ decays is based on the full reconstruction of one of the B mesons in the event, in the modes $B^+ \rightarrow D^{(*)0} h^+$ and $D^{(*)0} D_s^{(*)+}$ ($h = \pi, K$), selected in a sample of 275M $B\bar{B}$ events¹¹). Decays of the types $\tau \rightarrow \mu(e)\nu\bar{\nu}$, $\pi\nu$, $\pi\pi^0\nu$, and $\pi\pi\pi\nu$ are then searched for in the event remainders. The

¹A few weeks after this conference, the Belle collaboration has announced evidence for $B^+ \rightarrow \tau^+ \nu_\tau$ ¹⁰), thus providing the first evidence of a purely leptonic B decay and the first direct determination of the decay constant f_B .

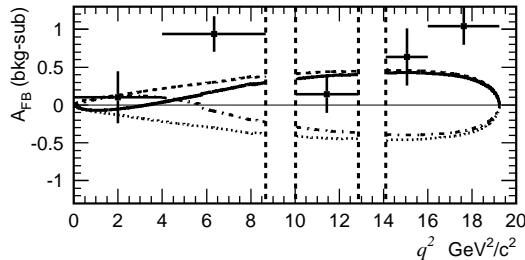


Figure 2: Fit result for the negative A_7 solution (solid) projected onto the background subtracted forward-backward asymmetry, and forward-backward asymmetry curves for several input parameters, including the effects of efficiency: A_7 positive case ($A_7 = 0.330$, $A_9 = 4.069$, $A_{10} = -4.213$) (dashed), A_{10} positive case ($A_7 = -0.280$, $A_9 = 2.419$, $A_{10} = 1.317$) (dot-dashed) and both A_7 and A_{10} positive case ($A_7 = 0.280$, $A_9 = 2.219$, $A_{10} = 3.817$) (dotted). The BSM scenarios shown by the dot-dashed and dotted curves are excluded by this measurement.

final event selection is based on the extra energy present in the electromagnetic calorimeter. So-called double-tag events (i.e. fully reconstructed $\Upsilon(4S)$ decays) are used to validate the simulation of this quantity. The resulting upper limit on the branching fraction is $\mathcal{B}(B^+ \rightarrow \tau^+ \nu_\tau) < 1.8 \times 10^{-4}$ at 90% CL. In the two-Higgs doublet model, this limit can be translated¹²⁾ in the exclusion of a region in the Higgs mass (m_{H^+}) versus $\tan \beta$ plane. The Belle result is shown in Figure 4 together with constraints placed by other measurements^{13, 14, 15)}.

3.2 $B^+ \rightarrow \mu^+ \nu_\mu$ and $B^+ \rightarrow e^+ \nu_e$

The electron and muon channels are studied in Belle by requiring one highly energetic lepton in the event and large missing energy and missing momentum corresponding to the undetected neutrino. All other particles in the event are used to reconstruct the companion B , which has to satisfy requirements on M_{bc} and ΔE . The final selection variable used to isolate the signal is the lepton momentum in the B rest frame, defined by the momentum of the recoiling companion B . The latest Belle results are $\mathcal{B}(B^+ \rightarrow \mu^+ \nu_\mu) < 2.0 \times 10^{-6}$ at 90% CL, based on a data sample of 140 fb^{-1} ¹⁶⁾ and $\mathcal{B}(B^+ \rightarrow e^+ \nu_e) < 5.4 \times 10^{-6}$ at 90% CL, based on 60 fb^{-1} ¹⁷⁾.

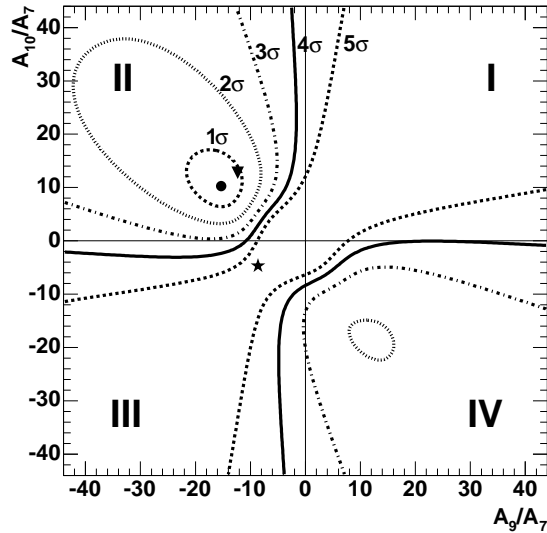


Figure 3: Confidence level contours for negative A_7 . Curves show 1σ to 5σ contours. The symbols show the fit (circle), SM (triangle), and A_{10} -positive (star) cases.

4 Search for $B^0 \rightarrow \ell^+ \ell^-$

The decay of B^0 to pairs of charged leptons can proceed in the SM via box diagrams or via annihilation into Z boson or photon. Similarly to their B^\pm counterparts, the predicted branching fractions are helicity suppressed for light leptons, down to about 10^{-10} for muons and 10^{-15} for electrons. Enhancements of these branching fractions are predicted by several BSM theories, such as high-tan β MSSM and some SUSY scenarios. The lepton flavour violating mode $B^0 \rightarrow e^\pm \mu^\mp$ is forbidden in the SM and so any signal in this mode would be an undeniable sign of new physics. Belle has set the following 90% CL upper limits based on a data sample of 78 fb^{-1} ¹⁸): $\mathcal{B}(B^0 \rightarrow \mu^+ \mu^-) < 1.6 \times 10^{-7}$, $\mathcal{B}(B^0 \rightarrow e^+ e^-) < 1.9 \times 10^{-7}$ and $\mathcal{B}(B^0 \rightarrow e^\pm \mu^\mp) < 1.7 \times 10^{-7}$. The latter result can be interpreted as a lower bound on the Pati-Salam leptoquark mass ¹⁹): $m_{LQ} > 46 \text{ TeV}/c^2$ at 90% CL.

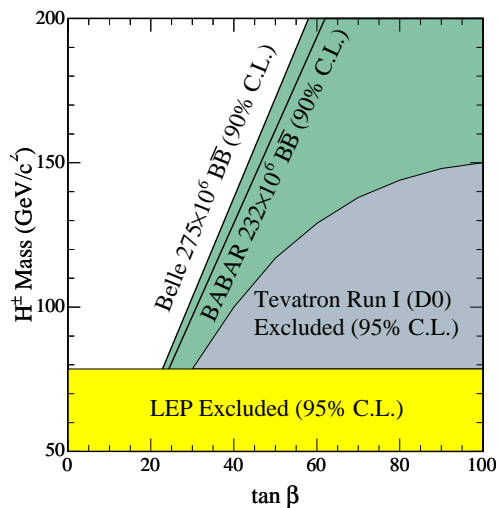


Figure 4: The 90% C.L. exclusion boundaries in the $[m_{H^+}, \tan \beta]$ plane obtained from the observed upper limit on $\mathcal{B}(B^+ \rightarrow \tau^+ \nu)$, compared with other experimental searches.

References

1. A. Abashian *et al.* (Belle Collaboration), Nucl. Instr. and Meth. A **479**, 117 (2002).
2. S. Kurokawa and E. Kikutani, Nucl. Instr. and Meth. A **499**, 1 (2003), and other papers included in this volume.
3. A. Ishikawa *et al.* (Belle Collaboration), hep-ex/0603018, submitted to Phys. Rev. Lett.
4. See, for example, G. Buchalla *et al.*, Rev. Mod. Phys. **68**, 1125 (1996).
5. H. H. Asatryan *et al.*, Phys. Lett. B **507**, 162 (2001).
6. E. Lunghi *et al.*, Nucl. Phys. B **568**, 120 (2000).
7. J. L. Hewett and J. D. Wells, Phys. Rev. D **55**, 5549 (1997); A. Ali *et al.*, Z. Phys. C **67**, 417 (1995); N. G. Deshpande *et al.*, Phys. Lett. B **308**, 322 (1993); B. Grinstein *et al.*, Nucl. Phys. B **319**, 271 (1991); W. S. Hou *et al.*, Phys. Rev. Lett. **58**, 1608 (1987).

8. D. A. Demir *et al.*, Phys. Rev. D **66**, 034015 (2002).
9. A. Ali *et al.*, Phys. Rev. D **66**, 034002 (2002).
10. K. Ikado *et al.* (Belle Collaboration), hep-ex/0604018, submitted to Phys. Rev. Lett.
11. K. Abe *et al.* (Belle Collaboration), hep-ex/0507034.
12. W. S. Hou, Phys. Rev. D **48**, 2342 (1993).
13. P. Bock *et al.* (ALEPH, DELPHI, L3 and OPAL Collaborations), CERN-EP-2000-055.
14. V. M. Abazov *et al.* (D0 Collaboration), Phys. Rev. Lett. **88**, 151803 (2002).
15. B. Aubert *et al.* (BaBar Collaboration), Phys. Rev. D **73**, 057101 (2006).
16. K. Abe *et al.* (Belle Collaboration), hep-ex/0408132.
17. K. Abe *et al.* (Belle Collaboration), Belle-conf-0247, available on the server <http://belle.kek.jp/>.
18. M.-C. Chang *et al.* (Belle Collaboration), Phys. Rev. D **68**, 111101 (2003).
19. J.C. Pati and A. Salam, Phys. Rev. D **10**, 275 (1974); A.V. Kuznetsov and N.V. Mikheev, Phys. Lett. B **329**, 295 (1994); G. Valencia and S. Willenbrock, Phys. Rev. D **50**, 6843 (1994).